PHYSICAL REVIEW B VOLUME 24, NUMBER 6 15 SEPTEMBER 1981

Pressure dependence of the optical properties and the band structure of the copper and silver halides

S. Ves,* D. Glötzel, and M. Cardona
Max-Planck-Institut für Festkörperforschung, 7 Stuttgart 80, Federal Republic of Germany

H. Overhof
Universität-Gesamthochschule Paderborn, 4790 Paderborn, Federal Republic of Germany

(Received 23 February 1981)

The absorption edge of CuCl, CuBr, CuI, and AgI is investigated with a diamond anvil cell as a function of pressure up to 16 GPa. The measurements, which reflect the various phase transitions undergone by these materials, yield the pressure coefficients of the lowest gaps. Particular attention is paid to the high-pressure rocksalt modifications, which are shown to have an indirect absorption edge in contrast to the direct edge of the sphalerite phases. This fact results from the influence of the different lattice symmetries on the halogen-p—metal-d hybridization in the valence bands. In order to interpret the data quantitatively, we have performed self-consistent local-density calculations with the linear combination of muffin-tin-orbitals—atomic-sphere approximation method and non-self-consistent Korringa-Kohn-Rostoker calculations with the standard muffin-tin potential. The pressure coefficients so obtained agree reasonably with the experimental ones. The gaps obtained by the self-consistent potential (with no adjustable parameter) are about 2 eV smaller than the experimental ones, thus reflecting shortcomings of the local-density method for excitation properties.

INTRODUCTION

The copper halides CuCl, CuBr, and CuI crystallize under normal conditions in the zinc-blende structure and thus can be considered as the last member of the series of group IV, III-V, II-VI, and I-VII tetrahedral semiconductors. A basic feature, however, separates the copper halides from the other members of the mentioned family: The $3d$ electrons of the copper hybridize very heavily with the p-like valence electrons of the halogen, and thus the number of valence electrons per formula unit instead of 8 becomes 18. This fact considerably complicates the task of calculating the energy-band structure of these materials: The pseudopotential method, perhaps the most successful and practical method for obtaining the band structure of simple semiconductors, becomes inapplicable to treat materials with valence bands involving relatively strongly localized d electrons. A number of interesting properties of these materials, such as the negative spin-orbit splitting of the uppermost valence band of CuCl (Refs. 1 and 2), have their origin in the p-d admixture just mentioned.

The I-VII compounds are the most ionic members of the IV, III-V, II-VI, and I-VII family. Their ionicity $\simeq 0.7$ in Phillips's scale is very close to that which separates the zinc-blende from the rocksalt phases ($f \simeq 0.71$).[3] At this value of f the wurtzite structure also becomes possible. Consequently, a number of different modifications are expected for these materials if the external pressure and temperature conditions are varied.[4] The isoelectronic silver halides AgCl and AgBr, with a slightly higher f, crystallize in the rocksalt structure under normal conditions while AgI ($f = 0.77$) crystallizes in either rocksalt of zinc-blende modifications up to 0.7 GPa (at room temperature) and goes over to the rocksalt structure above 0.7 GPa. The zinc-blende—rocksalt transition has profound implications for the band structure of these materials: p and d electrons do not hybridize in the latter at $k = 0$ as a result of the inversion symmetry while, on the contrary, the hybridization is strong in zinc blende. The nature of the lowest optical-absorption edge is determined by this fact: It is direct in the

zinc-blende and wurtzite modifications and indirect in rocksalt.

The purpose of this paper is to investigate experimentally and theoretically the pressure-induced zinc-blende → rocksalt transition and its effect on the lowest absorption edge of CuCl, CuBr, CuI, and AgI. In the copper halides the zinc-blende → rocksalt transition does not occur directly upon the application of pressure: a number of intermediate phases of lower, noncubic symmetry are found before the materials attain the rocksalt structure at $\simeq$10 GPa. The absorption edges of these materials and their pressure dependence have also been determined experimentally. Moreover, their crystal structures are too complicated and not too well known for a theoretical treatment.

In order to calculate the band structure of materials with relatively localized *d*-valence electrons it is most convenient to use techniques which emphasize the atomic nature of the wave functions. Among these techniques we have chosen here non-self-consistent Korringa-Kohn-Rostoker muffin-tin potential calculations, known to yield good results for the closely related II-VI compounds,[5] and fully self-consistent local-density calculations with the linear combination of muffin-tin-orbitals—atomic-sphere approximation (LMTO-ASA) (Ref. 6) method. The former technique was used in its relativistic version so as to include spin-orbit interaction, an effect of paramount interest when *p*-*d* hybridization occurs. (The spin-orbit splitting of the top valence band changes sign from CuCl to CuBr. This changes the symmetry of the top of the valence band[2]). All four compounds under consideration in their zinc-blende and rocksalt modifications were treated with this method. Only CuCl in the same two modifications was calculated with the semirelativistic version of the LMTO-ASA technique. All calculations were performed with the lattice constant corresponding to the lowest pressure at which they were found and with a slightly smaller (1 to 2%) lattice constant so as to obtain the volume dependence of the band structure, and thus the deformation potentials of the most important high-symmetry electronic states. A comparison of the experimentally observed pressure dependence of the absorption edges with the calculated band structures enables us to assign these absorption edges to definite transitions between valence and conduction bands.

EXPERIMENTS

Optical-absorption data were taken at high pressures up to 16 GPa for copper halides and to 8.5 GPa for AgI in a gasketed diamond anvil cell.[7,8] The procedure used has been described elsewhere.[9] Because of reactivity of our samples with the standard transmission fluids (methanol-ethanol mixtures) we omitted the fluid, filling the cell almost completely with the sample material. We found from the shape of the R_1 and R_2 lines of ruby imbedded in our sample that the pressure distribution was quite hydrostatic: No sign of broadening of the R_1 and R_2 lines was observed up to 10 Gpa. We have also used NaCl as a pressure transmitting medium, but this did not result in any improvement of the pressure distribution in the cell.

The first-order phase transitions in all these compounds can be observed visually with a low-power microscope.[10,11] In some cases they are sluggish and in others abrupt. The coexistence of both phases is indicated by the shaded area in the figures to follow.

For the determination of the absorption coefficients from transmittance data we used the sample thickness measured after pressure release. They were found to be 30 to 40 μm. We have used these values to calculate the absorption coefficients while being aware of the fact that the samples are somewhat thicker in the low-pressure range. A slight overestimate of the absorption coefficients in the low-pressure runs may then result.

Figure 1 is reproduced for completeness from

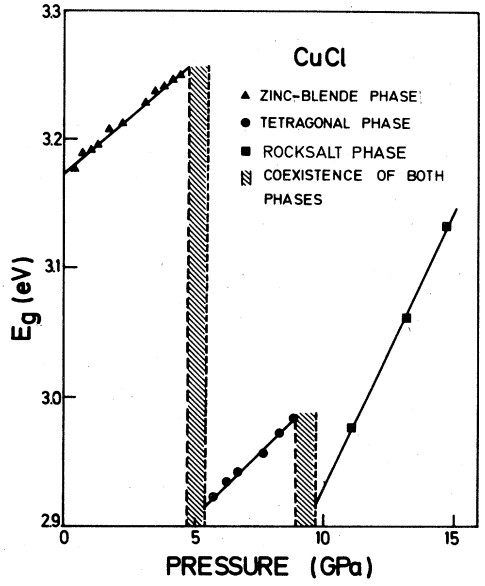

FIG. 1. Pressure dependence of the absorption edge of CuCl. The discontinuities at 5.0 and 9.0 GPa correspond to the phase transitions: zinc blende → tetragonal → rocksalt.

Ref. 9. It displays the variation with pressure of the lowest direct gap of CuCl. Two phase transitions are apparent as discussed in Ref. 9.

In Figs. 2, 3, and 4 we show the absorption spectra obtained in the region of stability of the zinc-blende, rhombohedral, tetragonal and rocksalt-type phase for CuBr and of the rocksalt phase for AgI. (Absorption data for AgI in the zinc-blende and wurtzite modification have appeared in Ref. 2.)

As mentioned in the previous section the absorption coefficients in the low-absorption region may be somewhat overestimated as a result of errors in the sample thickness. The bending over of the curves at high absorption coefficients is produced by scattered light or light leakage in the sample and cell. The maximum absorption coefficient in the zinc-blende phases, at the exciton knee, should be $\sim 10^5$ cm^{-1} for all the compounds under consideration.[2] As in the case of CuCl no error in the pressure coefficients of gaps should result because of the cutting of the absorption curve somewhat below (0.08 eV) the exciton knee.[9]

In all samples measured the lowest absorption edge of the zinc-blende modifications is sharp, as corresponds to a direct edge. This edge remains as sharp in the tetragonal modification of CuCl (Ref. 9) and CuBr (Fig. 4). The rocksalt modifications are definitely broader in all materials measured (see,

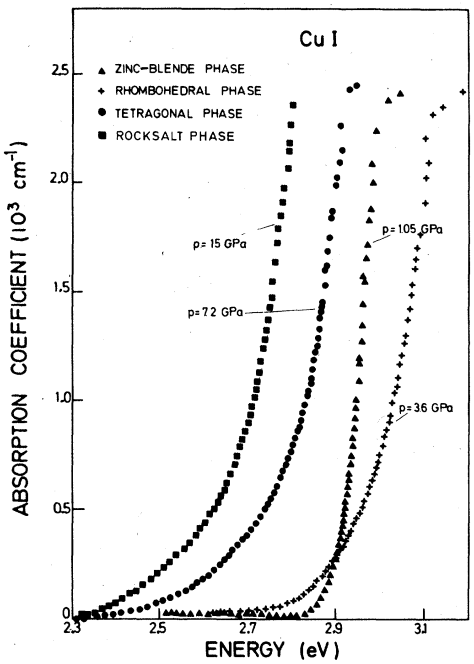

FIG. 3. Absorption coefficient of CuI for four crystallographic phases: zinc blende at 1.05 GPa (triangles), rhombohedral at 3.6 GPa (crosses), tetragonal at 7.2 GPa (circles), and rocksalt at 15 GPa (squares).

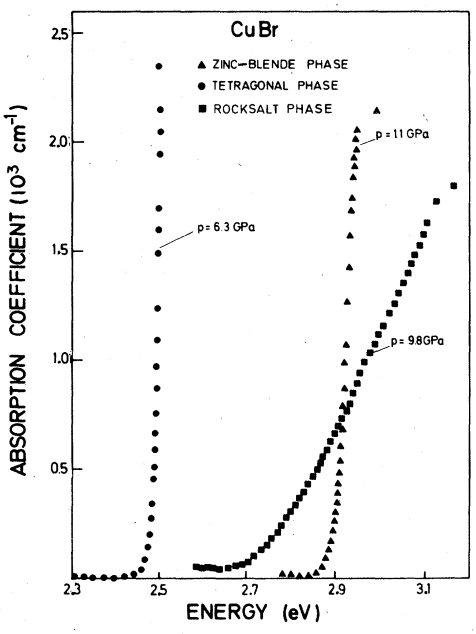

FIG. 2. Absorption coefficient of CuBr for three crystallographic phases: zinc blende at 1.1 GPa (triangles), tetragonal at 6.3 GPa (circles), and rocksalt at 9.8 GPa (squares).

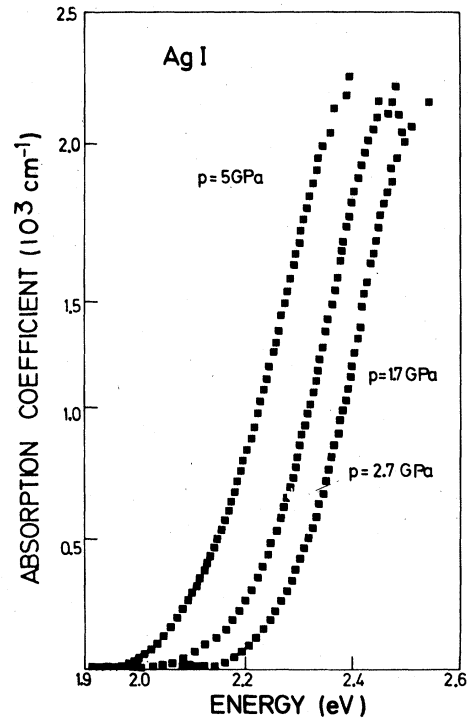

FIG. 4. Absorption coefficient of AgI in the rocksalt phase at pressures of 1.7, 2.7, and 5 GPa.

in particular, Fig. 2). As discussed in Ref. 9, we believe that this large width is evidence for an indirect lowest gap in all rocksalt modifications of the Ag and Cu halides. The edges of the rhombohedral and tetragonal phases of CuI (Fig. 3) also seem to be indirect. We lack, however, the theoretical underpinning for a firm assignment. In particular, we cannot discard the possibility of the broadening of the edge due to dichroism in optically anisotropic modifications.

In Figs. 1, 5, 6, and 7 we have plotted the energy gaps as a function of pressure for all the phases observed at room temperatures and under pressure in the cuprous halides as well as that of AgI in the NaCl modification. In the cases identified as *direct* gaps we defined the gap as the point of maximum absorption before *straight* light provokes an apparent saturation of the absorption edge ($\alpha \sim 2.5 \times 10^3$ cm^{-1}), one to two orders of magnitude lower in absorption coefficient than the exciton knee.[2] Comparison with published absorption curves at room temperature[2] and pressure [see Table I(a)] indicates that the gap so defined lies 80 to 100 meV below the exciton energy. We believe this small shift to lower absorption regions should not significantly affect the pressure coefficients obtained here.

In the case of rocksalt phaes we have estimated the indirect gap by plotting the square root of the absorption coefficient versus energy and extrapolating the resulting line to zero absorption (see Fig. 8 for AgI). The direct and indirect energy gaps determined in this manner are presented in Table I and are compared with other experimental values. The rocksalt modification of CuI may have two indirect edges as illustrated in Figs. 6 and 9.

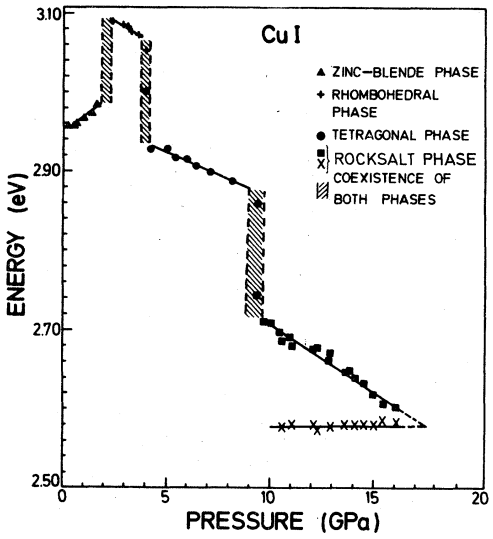

FIG. 6. Pressure dependence of the absorption edge of CuI. The discontinuities at 1.8, 4.6, and 9.0 GPa correspond to the phase transitions: zinc blende → rhombohedral → tetragonal → rocksalt. Note the existence of two absorption edges in the rocksalt phase as discussed in the text.

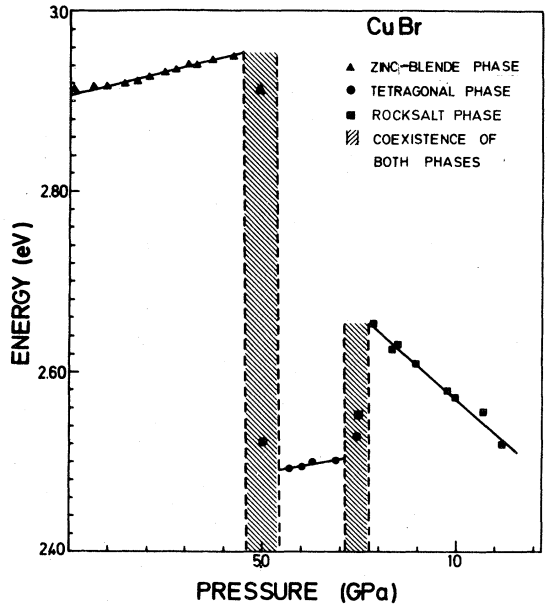

FIG. 5. Pressure dependence of the absorption edge of CuBr. The discontinuities at 5.0 and 7.5 GPa correspond to the phase transitions: zinc blende → tetragonal → rocksalt.

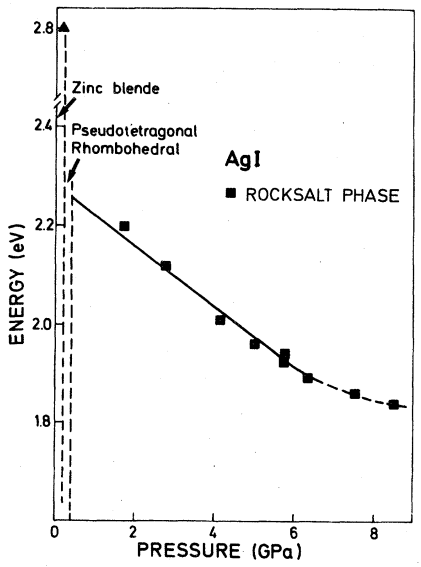

FIG. 7. Pressure dependence of the energy gap of AgI in the rocksalt phase.

TABLE I. (a) Energy gaps for CuCl, CuBr, CuI, and AgI, and deformation potentials in parentheses (in eV). (b) Pressure coefficients (meV/GPa) for the experimental energy gaps of (a), and observation pressure in GPa. Values without superscript are from this work. (NE stands for nonexistent.)

	Zinc blende (direct)	Rhombohedral (direct)	Tetragonal (direct)	Rocksalt (indirect)
	(a) Energy gaps and deformation potentials			
CuCl	3.17[a](−1)[a] 3.268[b](−0.4)[c,d]	NE	2.9[a](−1.65)[a]	3.0(−5.0)[a]
CuBr	2.91(−0.39)[e] 3.016[b](−0.2)[c]	NE	2.49(−0.45)	2.53(2.98)
CuI	2.95(−0.65)[e] 3.04[b](−1.0)[c]	3.09(0.6)	2.91(+0.61)	2.58(0) 2.70(1.41)
AgI	2.82 2.91[b]	NE		2.26(2.96)[h]
	(b) Pressure coefficients			
CuCl	17.8 at 0[a] 18.0 at 0[f] 9.0[c],7.0[d]	NE	21.0 at 5[a]	43.0 at 11[a] 0.0[d]
CuBr	10.0 at 0 4.0[c] −10. at 1[d]	NE	7.4 at 6 >0[d]	−37.1 at 11
CuI	19.2 at 0 29.0[c],41.0[d]	−14.8 at 3 −79.0[d]	−11.0 at 6 −61.0[d]	−19.3 at 11 −22.0[d]
AgI		NE		−61.0 at 0.5 −65.0[g]

[a]Reference 9.
[b]Reference 2.
[c]J. B. Antony, A. D. Brothers, and D. W. Lynch, Phys. Rev. B 5, 3189 (1974).
[d]A. L. Edwards and H. G. Drickamer, Phys. Rev. 122, 1149 (1961).
[e]Using compressibility data of Ref. 12.
[f]B. Batlogg and J. P. Remeika, Phys. Rev. Lett. 45, 1126 (1980).
[g]Reference 15.
[h]Using compressibility data of T. A. Fjeldly and R. G. Hanson, Phys. Rev. B 10, 3569 (1974).

In the noncubic phases the gaps have been defined in the same way as for the zinc-blende structure. The energy gap shifts to higher energies with pressure (blue shift) for cuprous halides in the zinc-blende phase and in the tetrahedral phase of CuCl and CuBr. In all other phases it shows a red shift with increasing pressure. The rates at which the gaps shift with pressure are listed in Table I(b).

From these pressure rates we have calculated the deformation potentials using the values of the bulk modulus given by Hanson *et al.*[12] for copper halides and the value given by Hinze[13] for AgI. For the high-pressure stable modifications of CuBr and CuI, we have estimated the bulk modulus by scaling the ambient pressure values with the relative change observed for CuCl.[10] This scaling works well in the case of AgI. In fact, by scaling the data of Ref. 12 for the zinc-blende phase of AgI we obtain $B \simeq 50$ GPa for the NaCl phase, very close to the measured value $B = 55$ Gpa (see Table I). This test supports the validity of the scaling procedure.

We have not seen any optical evidence for a metal-insulator transition in CuCl up to a pressure of 15 GPa but we observed darkening of the sample when exposed to laser radiation (5.14.5 nm) while carrying out pressure experiments on the zinc-

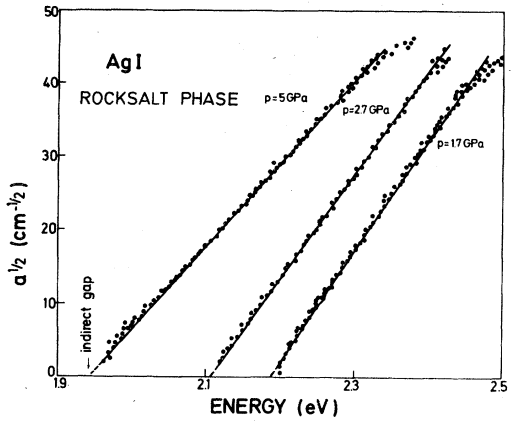

FIG. 8. Square root of the absorption coefficient for AgI in the rocksalt phase at 1.7, 2.7, and 5 GPa. Linear extrapolation to zero absorption yields the indirect absorption edge.

blende phase as reported by Chu *et al.*[14] We observed a similar phenomenon for CuBr: The sample appeared to fill with dark brown filaments upon laser illumination. In some samples the filaments were preserved in all pressure-induced phases. The filaments, however, disappeared after a period of about ten days, and only at the point where the ruby chip was placed, a small dark spot remainded.

We have not observed such darkening in CuI. The AgI sample becomes reddish immediately after transforming into the rocksalt phase as corresponds to the low indirect gap of this phase. The reddish tinge disappears as the pressure is released.

In Fig. 7 we show the shift of the "indirect" absorption edge of AgI with pressure in the rocksalt phase. The shift is linear up to 6 GPa. At higher pressures the gap versus pressure curve bends upwards, possibly an indication of an incipient transformation into the CsI phase, which, according to Drickamer,[15] should occur at 9.7 GPa.

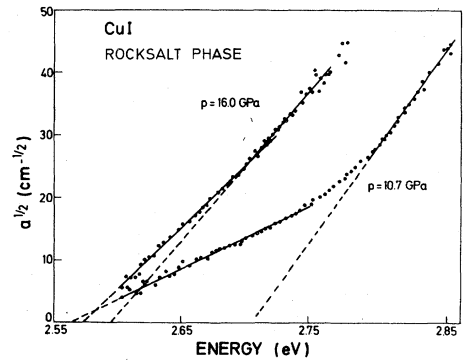

FIG. 9. Square root of the absorption coefficient for CuI in the rocksalt phase. At 10.7 GPa two linear regimes can be discriminated which yield two indirect absorption edges as displayed in Fig. 6.

THEORY

Since a quantitative *ab initio* theory of electronic excitations in extended systems does not yet exist, we employed two independent approximate band-structure approaches to this problem:

(1) Non-self-consistent relativistic calculations using the usual superposition potential and full Slater exchange for all studied materials.

(2) Self-consistent, semirelativistic local-density-functional[16] calculations for a few model substances.

Both approaches have their weaknesses as regards excitation energies. The success of the simple *ad hoc* potentials with a "proper" choice of atomic configurations has been well documented although it has never been fully understood. The local-density-functional theory is well founded for the ground state and adequate to investigate, e.g., structural stability and cohesive properties, but the one-particle energies may not be strictly interpreted as excitation energies. From previous work on insulators and semiconductors (see Ref. 17 and references therein) we know that energy gaps, as defined by these one-particle energies, are systematically underestimated by as much as 2 eV for, e.g., diamond. On the other hand, the only proper way to calculate deformation potentials is a self-consistent treatment, which includes the response of the electronic system to the change of atomic volume and its effect on the crystal potential. Nevertheless, considerable success has been also obtained in calculating deformation potentials with non-self-consistent techniques through a "judicious" choice of the dependence of the potential on pressure.[18]

The non-self-consistent calculations were performed with the relativistic KKR method, where, particularly, in the open sphalerite structure the interstitial (flat potential) region was rather large, since touching muffin-tin spheres filled only 34% of the unit cell. The potential was constructed from a superposition of ionic charge densities, and the interstitial potential constant was determined by the proper average. For the self-consistent calculations we used the linear-muffin-tin-orbital (LMTO) method in the atomic-sphere approximation (ASA).[6] In order to improve the space filling and the representation of the potential we introduced additional interstitial spheres in the octahedral (tetrahedral) sites of the

ZnS (NaCl) structure, which results in a considerably improved space filling of 68% (like in the bcc structure). Details of this method, as well as an account of the cohesive properties of CuCl will be given in a forthcoming publication.[19] Glötzel, Segall, and Anderson[17] have recently tested the accuracy of this device for the elemental semiconductors Si, Ge, and diamond. They were able to account for the cohesive properties of these systems and also obtained detailed agreement with the best self-consistent state-of-the-art band calculations. This gives us some confidence, that the major part of the non-muffin-tin effect is provided by the introduction of interstitial spheres. Part of the discrepancies in the calculated deformation potentials with the non-self-consistent (KKR) method and the self-consistent LMTO method, to be discussed below, might be attributed to the poor space filling in the former method. We restricted the calculations to the initial zinc-blende structure and the high-pressure rocksalt structure, common to the Cu halides and AgI for obvious reasons (the other structures are too complicated). Table II reproduces the lattice constants used in the calculations. KKR calculations of the zinc-blende phases have recently been published by one of the authors[20,21] and are not reproduced here. The KKR band structures along the high-symmetry directions for the rocksalt modifications of CuCl, CuBr, CuI, and AgI are shown in Figs. 10(a)–10(d). Because of the large computational effort required we only performed self-consistent calculations (with the LMTO method) for CuCl in both phases and the rocksalt phase of AgCl. The results are displayed in Figs. 12–14. Of the valence bands we show only those composed of the halogen-p and metal-d orbitals; the much lower s bands of the halogen ions are omitted as they are not relevant to the present discussion.

The effect of halogen-p – metal-d hybridization on the electronic structure of CuCl is illustrated in Fig. 11, which shows the self-consistent energy bands with (solid) and without (dashed) p-d hybridization

TABLE II. Lattice constants (a.u.) used in the band-structure calculations for the Ag and Cu halides.

	Rocksalt		Zinc blende
	Ag	Cu	Cu
Cl	10.46	9.373	10.23
Br	10.92	9.71	10.76
I	11.47	9.73	11.72

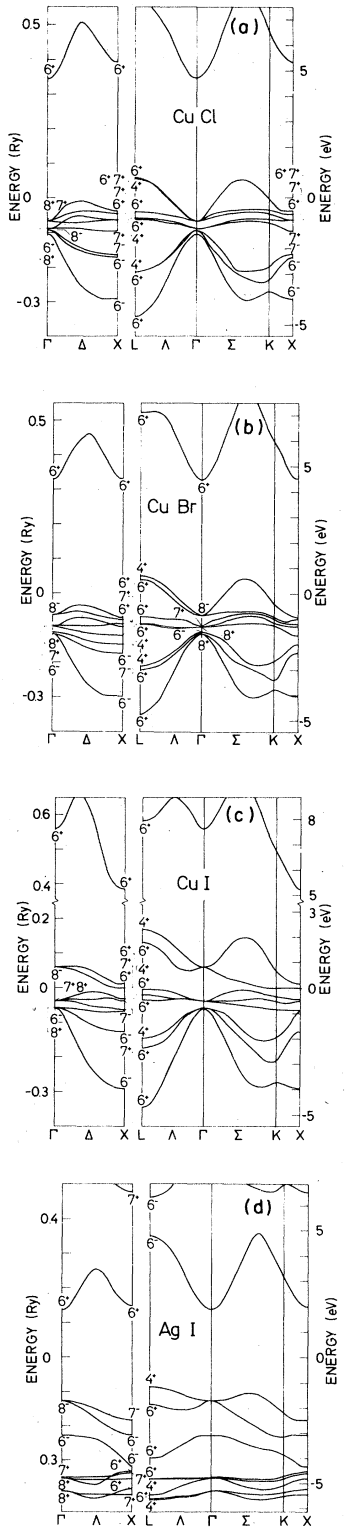

FIG. 10. Relativistic band structures of the Cu and Ag halides in the rocksalt phase, obtained from a standard muffin-tin potential with the KKR method. (a) CuCl, (b) CuBr, (c) CuI, and (d) AgI.

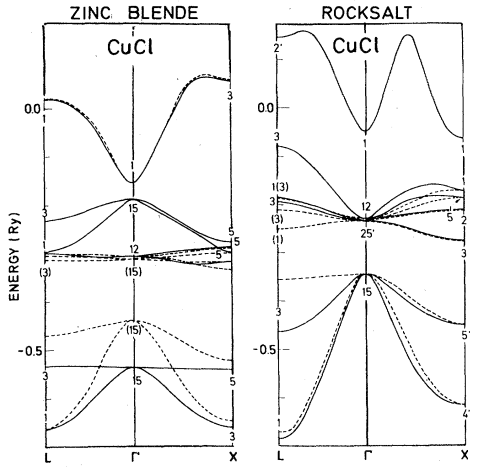

FIG. 11. Semirelativistic band structures of CuCl in the zinc-blende phase (left panel) and the rocksalt phase (right panel) obtained from a self-consistent local-density potential with the LMTO-ASA method. Dashed lines indicate results without halogen-p and metal-d hybridization.

for both phases at their respective lattice constant. The p and d valence bands hybridize strongly throughout the Brillouin zone except at the Γ point ($\vec{k}=0$), where the p-d interaction is forbidden as a result of the inversion symmetry of the rocksalt structure (right panel of Fig. 11). Hence the d bands, unmixed at $k=0$, begin to mix as $\vec{k}$ increases along any direction. As a result, a strong repulsion between the p and d bands takes place off $\vec{k}=0$, with the effect that the top of the valence band does not occur at Γ. High valence-band maxima occur at L and in the middle of the Σ directions. The conduction bands are largely unaffected by this mixing with nearly degenerate lowest minima at the Γ and X points. Consequently, the lowest absorption edge must become indirect either from L or Σ to Γ or X.

This state of affairs is completely different to that which prevails in the zinc-blende modifications of these compounds (for CuCl see left panel of Fig. 11). In this modification the inversion symmetry is absent and p-d mixing is allowed even at Γ. The top of the valence band thus remains at the Γ point as in all conventional tetrahedral semiconductors (e.g., Ge, GaAs, ZnSe); the lowest absorption edge of these materials remains direct,[2] in spite of erroneous statements to the contrary in the literature[22,23] (in Ref. 22 an indirect gap of about 0.3 eV is postulated to explain anomalies in the lattice dynamics of CuCl. In Ref. 23 a direct gap of 0.8 eV is obtained in calculations and experiments. Such a gap would make the sample black in the visible, and thus could not be correct).

Before we proceed to the comparison with experiment, we want to discuss the self-consistent band results. In Figs. 12 to 14 we display the band structure of CuCl in both phases and of AgCl in the rocksalt phase, along with the band structures for a slightly reduced constant (by 2, 1.2, and 2%, respectively) aligned at the twofold degenerate d level Γ_{12}. The regions, where the band energies drop with respect to Γ_{12} under compression, are shaded (deformation potential $D \equiv dE/d\ln V > 0$) and those with a negative deformation potential are left open. By inspection of Fig. 13 we find, e.g., that for the $L \rightarrow \Gamma$ transition $D < 0$, and for the $L \rightarrow X$ transition $D > 0$.

The conduction-band minima of the NaCl phases at X and Γ are rather close in CuCl, whereas in AgCl (Fig. 14) the X_1 state is considerably higher in energy. The Γ_1 state is a pure s state, whereas the X_1 state has a 20% admixture of halogen-d character and is essentially the bottom of the nonmetal-d band. Therefore, the X_1 state is shifted to lower energies proportional to the width of the nonmetal-d band, which increases either with increasing atomic number (Cl→Br→I) or under compression. For the Cu compounds this shift is demonstrated in Figs. 10(a), 10(b), and 10(c), where the corresponding relativistic level X_6^+ moves down with respect to Γ_6^+.

A number of band-structure calculations for

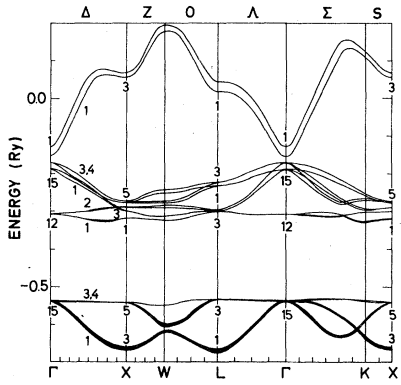

FIG. 12. Semirelativistic band structure of CuCl in the zinc-blende phase obtained from a self-consistent local-density potential with the LMTO-ASA method. Band structures are displayed for the observed lattice constant (see Table II) and a 2% reduced lattice constant. The area between corresponding bands is shaded (left open) if the deformation potential $D \equiv dE/d\ln V$ is positive (negative).

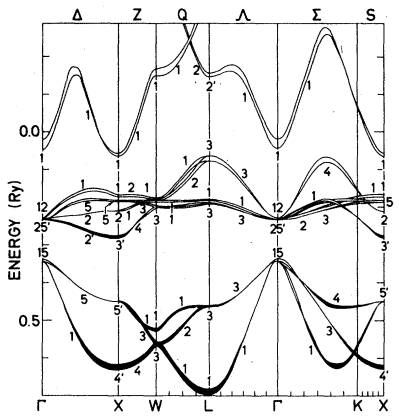

FIG. 13. Semirelativistic band structure of CuCl in the rocksalt phase obtained from a self-consistent local-density potential with the LMTO-ASA method. Band structures are displayed for the observed lattice constant (see Table II) and for a 1.2% reduced lattice constant. The area between corresponding bands is shaded (left open) if the deformation potential is positive (negative).

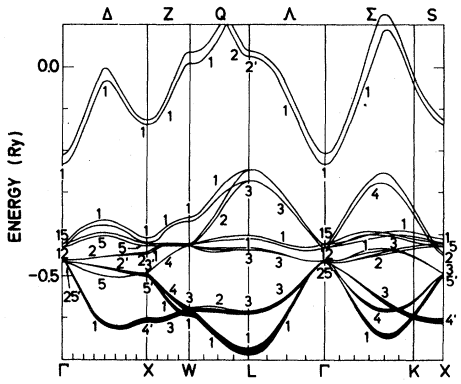

FIG. 14. Semirelativistic band structure of AgCl in the rocksalt phase, obtained from a self-consistent local-density potential with the LMTO-ASA method. Band structures are displayed for the observed lattice constant (see Table II) and a 2% reduced lattice constant. The area between corresponding bands is shaded (left open) if the deformation potential is positive (negative).

zinc-blende CuCl have recently been reported which employ different techniques: LCAO (Ref. 24) and Hartree-Fock (Ref. 25), KKR (Refs. 21 and 26) and LMTO (Ref. 27), and different potential prescriptions. In Tables III (a) and III (b) we compare the lowest direct energy gap and corresponding deformation potential, as obtained from these calculations, with our present KKR and LMTO results. The KKR calculation of Overhof,[21] using the standard potential, agrees well with the very similar calculation of Doran and Woolley[26]; and our self-consistent local-density LMTO calculation supports the very small gap of 0.8 eV found by Freeman and co-workers[27] with a similar technique. The gap of 2.0 eV found by Zunger and Cohen[24] seems somewhat large for a self-consistent local-density calculation and has been criticized by Kleinman and Mednick,[25] who attribute this fact to the use of an incomplete LCAO basis set.

In Tables IV (a) and IV (b) we display our theoretical results for the lowest direct and indirect energy gaps and deformation potentials or the Cu and Ag halides in the rocksalt modification along with literature data. Previous calculations for the silver halides[28–30] have been adjusted to agree with one experimentally observed energy gap and, therefore, may not be directly compared with our essentially parameter-free approach.

The gap between the rather localized $3d$ or $4d$ valence band and the broad s-like conduction band in these compounds is very sensitive to the approxi-

TABLE III. Comparison of calculated lowest direct energy gap and deformation potentials for zinc-blende CuCl (in eV).

	This work		References					
	KKR	LMTO	a	b	c	d	e	f
Gap	3.21	0,5	3.09	2.0	2.33	0.8	3.1	3.44
Deformation potential	−0.3	−1.8	−2.2	−2.2				+0.3

[a]A. Zunger and M. L. Cohen, Phys. Rev. B 20, 1189 (1979).
[b]L. Kleinman and K. Mednick, Phys. Rev. B 20, 2487 (1979).
[c]Kong-Sop Song, J. Phys. Chem. Solids 28, 2003 (1967).
[d]A. J. Freeman, C. S. Wang, T. Jarlborg, M. Weinert, F. Wagner, and C. W. Chu, Intern. J. Quantum Chem., Symp. 13, 445 (1979).
[e]N. J. Doran and A. M. Woolley, J. Phys. C 12, L321 (1979).
[f]E. Calabrese and K. B. Fowler, Phys. Status Solidi B 57, 135 (1973).

TABLE IV. (a) Comparison of calculated energy gaps for the rocksalt phases of the Cu and Ag halides (in eV). (b) Comparison of calculated deformation potentials for the gaps of (a) (in eV). Values without superscript are from this work, standard potential KKR calculation.

	Direct $\Gamma\rightarrow\Gamma$	Indirect $L,\Sigma\rightarrow\Gamma$	Indirect $L,\Sigma\rightarrow X$
		(a) Energy gaps	
CuCl	5.64, 2.5[a]	L:3.97, 0.6[a] Σ:4.0, 0.5[a]	L:4.59, 0.1[a] Σ:4.62, 0.2[a]
CuBr	5.33	L:3.79 Σ:3.95	L:3.99 Σ:4.15
CuI	6.79	L:5.32 Σ:5.65	L:2.96 Σ:3.29
AgCl	4.21, 5.13,[b] 5.47[c] 5.17,[d] 2.7[a]	L:3.19, 3.71,[c] 3.28[b] 0.5,[a] 3.17[d] Σ:3.25, 0.6[a]	L:4.9, 6.6,[d] 1.8[a] Σ:4.95, 1.9[a]
AgBr	3.69, 4.29,[b] 4.22[c]	L:2.94, 2.89,[b] 3.23[c] Σ:3.05	L:4.4 Σ:4.22
AgI	3.59	L:3.04 Σ:3.30	L:3.20 Σ:3.46
		(b) Deformation potentials	
CuCl	−7.3, −9[a]	L:−4.7, −4.3[a] Σ:−5.5, −4.5[a]	L:−1.0, 1.8[a] Σ:−1.8, 1.6[a]
CuBr	−9.7	L:5.2 Σ:5.1	L:−1.3 Σ−1.2
CuI	−11.7	L:−7.9 Σ:−8.2	L:1.2 Σ:0.9
AgCl	−6.3, −4.2[c] −3.7[a]	L:−2.6, 0.1[c] 0.1[a] Σ:−2.3, −0.7[a]	L:2.5,[a] −2.5 Σ:2.3,[a] −2.2
AgBr	−6.8	L:−3.8 Σ:−3.9	L:−3.5 Σ:−3.6
AgI	−7.6	L:−5.3 Σ:−5.8	L:−2.8 Σ:−3.2

[a]This work: self-consistent LMTO calculation.
[b]Reference 28.
[c]Reference 29.
[d]Reference 30.

mation used to describe exchange and correlation. Calculations employing the Slater exchange (exchange paramer $\alpha=1$) yield lower and narrower d bands and consequently much larger energy gaps (Refs. 21, 25, and 26), than local-density calculations (Ref. 27 and this work) with an approximate effective exchange coefficient $\alpha\simeq 0.7$.

DISCUSSION

In Table V we compare the calculated direct energy gaps and deformation potentials of the zinc-blende modifications with the experimental values of Table I. The latter were obtained from calculations with the equilibrium lattice constant at zero pressure

TABLE V. Comparison of experimental and calculated direct energy gaps in the zinc-blende phase (in eV); deformation potentials in parentheses.

		Potential	
	Expt.	Superposition Slater exchange	Self-consistent local density
CuCl	3.17(−1)	3.2(−0.3)	0.5(−1.8)
CuBr	2.91(−0.39)	3.1(−0.5)	
CuI	2.95(−0.65)	3.5(−0.7)	
AgI	2.82	3.3(−7.6)	

(a_0) and with a lattice constant $a=0.99a_0$. The muffin-tin potential V_0 was taken, in all cases, to be the average crystal potential $V_0=\bar{V}_0(a)$ in the flat muffin-tin region. The non-self-consistent KKR results are all close to 3 eV as are the experimental ones, and the deformation potentials are consistently small and negative. The local-density value for the gap of CuCl (0.5 eV) is much too small, whereas the deformation potential agrees well with experiment.

When comparing the indirect gaps of the rocksalt modifications (Table VI) one finds again gaps that are far too small in the self-consistent calculation. The lowest indirect gap of CuCl is calculated to be 3.97 for the $L\rightarrow\Gamma$ transition with the standard potential sufficiently close in view of computational uncertainties to the measured 3 eV. The deformation potential calculated non-self-consistently for these transitions (see Table IV) is −4.7 eV, in excellent agreement with the measured value [−5 eV, Table I(a)]. The local-density potential, in spite of yielding incorrect energy gaps, gives also a reasonable value for this deformation potential (−4.3 eV). We thus assign the indirect gap observed for the NaCl phase of CuCl to $L\rightarrow\Gamma$ "allowed" indirect transitions.

We discuss next the indirect gap of the NaCl phase of CuBr for which material only the KKR calculations are available. The measured energy of this gap (2.53 eV) is compatible with any of the four nearly degenerate calculated indirect gaps listed in Table IV. Its deformation potential, however, is +2.98 eV and has the opposite sign to that measured for CuCl. We note (Table VI and Fig. 10) that the X minimum of the conduction band drops down with respect to the Γ minimum through the sequence CuCl → CuBr → CuI, which results from the lowering and broadening of the halogen d bands.

This fact, coupled with the drastic change in the measured deformation potential of the indirect gap between CuCl and CuBr, suggests that the lowest edge changes from one involving a final state at Γ to one in which the final state is at X. The two most likely possibilities are $L\rightarrow X$ and $\Sigma\rightarrow X$. The KKR calculations yield for both those gaps ~4 eV in CuBr, 3 eV in CuI, with $L\rightarrow X$ slightly lower than $\Sigma\rightarrow X$. The deformation potential calculated for the $L\rightarrow X$ gap of CuCl with the LMTO method is +1.8 eV, and it is expected to remain nearly the same for CuBr and CuI. This deformation potential is sufficiently close that measured for the indirect gap of the NaCl phase in CuBr (1.41 eV) and CuI (2.96 eV) to make the assignment of the indirect gap to $L\rightarrow X$ transitions. The less likely $\Sigma\rightarrow X$ possibility, however, cannot be completely discarded. In particular, in the rocksalt phase of CuI, as we mentioned previously, both of the possibilities $L\rightarrow X$ and $\Sigma\rightarrow X$ seem to appear (see Figs. 6 and 9). The gap is composed obviously of two components. As the pressure is increased to 16 GPa, the two gaps seem to become one. The lower one of these two gaps seems to have a zero pressure coefficient (see Fig. 6). At about 17.5 GPa both gaps should have the same value. Comparing the calculated deformation potentials listed in Table IV and following the same argumentation as for CuBr it is logical to attribute the one that shifts with pressure as an $L\rightarrow X$ and that which does not show any pressure shift as a $\Sigma\rightarrow X$ transition.

We discuss next the rocksalt modification of AgI which, according to Table I, has an indirect gap of 2.26 eV. For the same reason as in the copper halides, the conduction-band minimum at X drops throughout the sequence AgCl-AgBr-AgI. In AgCl and AgBr, stable at room temperature in the rocksalt modifications, the indirect gap is $L\rightarrow\Gamma$.[30] We calculate for this gap in AgCl a deformation potential of −2.6 eV (Table IV) as compared to the measured value of 0.6 eV (Ref. 31), which nevertheless agrees better with the calculation of Fowler (+0.1

TABLE VI. Comparison of experimental and calculated indirect energy gaps and deformation potentials of the Cu and Ag halides in the rocksalt phase (in eV).

	Expt.	Transition	Superposition potential	Self-consistent LD
CuCl	3.0(−5)[a]	$L\rightarrow\Gamma$	4.0(−4.7)	0.6(−4.3)
		$\Sigma\rightarrow\Gamma$	4.0(−5.5)	0.5(−4.5)
		$L\rightarrow X$	4.6(−1.0)	0.1(1.8)
		$\Sigma\rightarrow X$	4.6(−1.8)	0.2(1.6)
CuBr	2.53(+3)[a]	$L\rightarrow\Gamma$	3.8(−5.2)	
		$\Sigma\rightarrow\Gamma$	3.95(−5.1)	
		$L\rightarrow X$	4.0(−1.3)	
		$\Sigma\rightarrow X$	4.1(−1.2)	
CuI	2.70(+1.4)[a]	$L\rightarrow\Gamma$	5.3(−7.9)	
		$\Sigma\rightarrow\Gamma$	5.65(−8.2)	
		$L\rightarrow X$	3.0(1.2)	
		$\Sigma\rightarrow X$	3.3(0.2)	
AgCl	3.62(0.65)[b]	$L\rightarrow\Gamma$	3.2(−2.6)	0.5(0.1)
	(0.51)[c]	$\Sigma\rightarrow\Gamma$	3.25(−2.3)	0.6(−0.1)
		$L\rightarrow X$	4.9(−2.5)	1.8(2.5)
		$\Sigma\rightarrow X$	4.95(−2.2)	1.9(2.3)
AgBr	3.05(0.68)[b]	$L\rightarrow\Gamma$	2.94(−3.8)	
	(0.2)[c]	$\Sigma\rightarrow\Gamma$	3.05(−3.9)	
		$L\rightarrow X$	4.4(−3.5)	
		$\Sigma\rightarrow X$	4.22(−3.6)	
AgI	2.26(2.96)[a]	$L\rightarrow\Gamma$	3.04(−5.3)	
		$\Sigma\rightarrow\Gamma$	3.30(−5.8)	
		$L\rightarrow X$	3.20(−2.8)	
		$\Sigma\rightarrow X$	3.50(−3.2)	

[a]Present work.
[b]A. D. Brothers and D. W. Lynch, Phys. Rev. 180, 911 (1969).
[c]R. B. Aust, Phys. Rev. 170, 784 (1968).

eV) (Ref. 29) and our self-consistent result (+0.1 eV). We thus believe our KKR calculation for the deformation potentials of the gaps of the silver halides to be biased towards the negative side. If this assumption is correct, our data would be consistent with an $L\rightarrow X$ gap for which we calculate a deformation potential of −2.8 eV in AgI. This number is to be compared with the experimental one of +2.96 eV.

It is interesting to point out that the *indirect* gaps of the NaCl modifications are nearly the same as the *direct* ones of the zinc-blende phases; the direct gaps of the rocksalt modification are much higher. This can be understood if one associates a shrinkage of the gaps to the p-d mixing (and mutual repulsion of the valence bands). This shrinkage would then be the same regardless of whether it was produced by the lack of inversion symmetry at Γ (direct gaps of zinc-blende phases) or by the crystal field off $\vec{k}=0$ (indirect gaps of rocksalt phases).

ACKNOWLEDGMENTS

We would like to thank O. K. Andersen, B. Segall, D. Hochheimer, and A. Jayaraman for stimulating discussions. Technical assistance of W. Dieterich with the high-pressure equipment is gratefully acknowledged. S. V. would like to thank the DAAD for the award of a fellowship.

*On leave from the University of Thessaloniki, Greece.
[1]For a review see A. Goldman, Phys. Status Solidi 81, 9 (1977).
[2]M. Cardona, Phys. Rev. 129, 69 (1963); see also R. Coelho, Report NONR Contract No. 1841 (10), Massachusetts Institute of Technology (unpublished).
[3]J. C. Phillips, *Bonds and Bands in Semiconductors* (Academic, New York, 1973).
[4]V. Meisalo, M. Kalliomäki, High Temp.—High Pressures 5, 663 (1973).
[5]P. Eckelt, O. Madelung, and J. Treusch, Phys. Rev. Lett. 18, 656 (1967).
[6]O. K. Andersen, Phys. Rev. B 12, 3060 (1975).
[7]G. J. Piermarini, S. Block, J. D. Barnett, and R. A. Forman, J. Appl. Phys. 46, 2774 (1975).
[8]B. Welber, M. Cardona, C. K. Kim, and S. Rodriguez, Phys. Rev. B 12, 5729 (1975).
[9]H. Müller, S. Ves, H. D. Hochheimer, and M. Cardona, Phys. Rev. B 22, 1052 (1980).
[10]G. J. Piermarini, F. A. Mauer, S. Block, A. Jayaraman, J. H. Geballe, and G. W. Hull, Jr., Solid State Commun. 32, 275 (1979).
[11]A. Van Valkenburg, J. Res. Nat. Bur. Stand. 68A, 97 (1964).
[12]R. C. Hanson, J. R. Hallberg, and C. Schwab, Appl. Phys. Lett. 21, 490 (1972).
[13]E. Hinze, High Temp.—High Pressures 1, 53 (1969).
[14]C. W. Chu and H. K. Mao, Phys. Rev. B 20, 4474 (1979).
[15]H. G. Drickamer, in *Solid State Physics,* edited by F. Seitz and D. Turnbull, Vol. 17 (Academic, New York, 1965), p. 1.
[16]L. Hedin and B. I. Lundqvist, J. Phys. C 4, 2064 (1971); U. von Barth and L. Hedin, J. Phys. C 5, 1629 (1972).
[17]D. Glötzel, B. Segall, and O. K. Andersen, Solid State Commun. 43, 403 (1980).
[18]F. Cerdeira, J. de Witt, U. Rössler, and M. Cardona, Phys. Status Solidi B 41, 735 (1970).
[19]O. K. Andersen and D. Glötzel (unpublished).
[20]H. Overhof, J. Phys. Chem. Solids 38, 1214 (1977).
[21]H. Overhof, Phys. Status Solidi B 97, 267 (1980).
[22]A. P. Rusakov, Phys. Status Solidi B 72, 503 (1975).
[23]A. J. Freeman, T. Jarlborg, and M. Weinert, Bull. Am. Phys. Soc. 24, 498 (1979); A. J. Freeman, F. Wagner, Jr., and M. Weinert, *ibid.* 24, 498 (1979)
[24]A Zunger and M. L. Cohen, Phys. Rev. B 20, 1189 (1979); L. Kleinman and K. Mednick, *ibid.* 20, 2487 (1979); E. Calabrese and K. B. Fowler, Phys. Status Solidi B 57, 135 (1973); Kong-Sop Song, J. Phys. Chem. Solids 28, 2003 (1967).
[25]A. B. Kunz and R. S. Weidman, J. Phys. C 12, L371 (1979).
[26]N. J. Doran and A. M. Wooley, J. Phys. C 12, L321 (1979).
[27]A. J. Freeman, C. S. Wang, T. Jarlborg, M. Weinert, F. Wagner, and C. W. Chu, Intern. J. Quantum Chem. Symp. 13, 445 (1979); F. Herman and R. V. Kasowski, private communication.
[28]P. M. Scop, Phys. Rev. 139, A934 (1965),
[29]A. B. Fowler, Phys. Status Solidi B 52, 591 (1972).
[30]J. Shy-Yih Wang, M. Schlüter, and M. L. Cohen, Phys. Status Solidi B 77, 295 (1976).
[31]A. D. Brothers and D. W. Lynch, Phys. Rev. 180, 911 (1969).